Condensed Matter Theories
Volume 13

ISBN 1-56072-602-4

CHARGED METAL CLUSTERS: ATOMISTIC VERSUS CONTINUOUS BACKGROUND DESCRIPTIONS

F. Nogueira, A. Vieira, M. Brajczewska, and C. Fiolhais
Department of Physics
University of Coimbra, P-3000 Coimbra, PORTUGAL

1. INTRODUCTION

Atomic clusters which are observed in mass spectrometers are charged. Simple models for the ions like the jellium model have allowed to understand the electronic shell structure of metal clusters. For instance, Na_3^+ is a magic cluster, characterized by an higher abundance in spectra and a relatively higher value of the ionization potential (second ionization of Na_3^+). Within the jellium model, the valence electrons move in a self-consistent field due to the continuous positive background and their own interaction. Major gaps in the single-particle spectrum explain magic electron numbers such as 8 in the above example. In more realistic models, the ions are localized at equilibrium positions which may be determined from quantum mechanical first principles considering either all the electrons or, a procedure which is much more effective, only the valence electrons interacting with the cores via electron-core potentials (pseudopotentials). It is a triumph of the jellium model that more sophisticated treatments of the ions do not alter many previous conclusions, e. g., the special stability of some clusters. That enhanced stability of some clusters and some other properties of simple metal clusters are therefore due to the weakly bound valence electrons and not to the ions whose main role is to neutralize all or almost all of the charge. Simple theories are indeed adequate for simple metals.

Considering clusters of increasing size, we may go over to the bulk limit. One of the goals of cluster physics is to know how bulk and surface properties emerge from the corresponding quantities in finite size systems (for instance, how the ionization potential leads, in the limit of big clusters, to the work function). An advantage of continuous background descriptions, as jellium, over atomistic ones is that the latter cannot handle very big clusters.

Here, we describe neutral and charged sp-bonded metal clusters, using different models of increasing complexity and realism for the ions. Starting from jellium, we continue with the Stabilized Jellium Model (SJM) or Structureless Pseudopotential Model, which introduces a constant potential inside the cluster as a perturbative improvement on jellium, go over to the Spherically Averaged Pseudopotential Model

(SAPS), where the ions are localized but, as a result of making a spherical average of the pseudopotential, are restricted to occupy spherical shells, and end up with an "ab initio" pseudopotential description (AIPM). For this one, and in order to deal with charged clusters, we use a modification of the standard plane-wave technique. In fact, this method for atomistic cluster calculations - where the clusters are placed inside supercells with periodic boundary conditions and a plane-wave basis is used to expand the orbits - is restricted in its usual form to neutral systems, due to the long-range interaction between a cluster and its periodic images. An adequate shielding must be provided in order to study charged objects.

The theoretical framework for all these approaches is density functional theory [1]. Given local pseudopotentials, the energy of the many valence-electron system is an universal functional of the one-body density. In the Kohn-Sham formulation, the unknown part of that functional is the exchange-correlation energy, for which normally the Local Density Approximation, LDA, is considered (recent semi-local approximations give an overall improvement for many atomic, molecular, and solid-state properties [2], but the exchange part still needs to be improved for a better account of surface properties). Minimization of the energy functional with respect to the density is equivalent to solving the Kohn-Sham equations, which are single-particle self-consistent equations.

Accepting the LDA, we will show in the next two sections some results of the Kohn-Sham equations using different external potentials: Jellium Model, Stabilized Jellium (Section 2), Spherically Averaged Pseudopotential Model and "Ab initio" Pseudopotential Model (Section 3). The conclusions are presented at the end. The material presented here is a short review of work recently done at the Center for Theoretical Physics, University of Coimbra, but the calculations for charged clusters with the plane-wave method are new.

2. CONTINUOUS BACKGROUND MODELS: JELLIUM AND STABILIZED JELLIUM DENSITY FUNCTIONALS

For simplicity, we consider clusters with spherical symmetry. The jellium functional of the valence electron density n and the background (fixed) positive density n_+ may be written as

$$E_J[n,n_+] = T[n] + E_{xc}[n] + \tfrac{1}{2}\int d^3r \int d^3r' \frac{n(\vec{r})n(\vec{r'})}{|\vec{r}-\vec{r'}|} + 4\pi \int r^2\, n(r)\, v_{ext}(r)\, dr + U_B[n_+] \qquad (1)$$

where $T[n]$ is the kinetic energy, $E_{xc}[n]$ is the exchange-correlation energy (in the LDA), v_{ext} is the jellium external potential, and the last term stands for the electrostatic background repulsion, which is $U_B[n_+] = \frac{3}{5}\frac{N^2}{R}$ for a spherical cluster with N electrons and radius $R = r_s N^{-1/3}$, r_s being the usual density parameter.

Since jellium has been extensively studied and applied in cluster physics [3] we present and discuss Stabilized Jellium [4]. Its density functional reads as

$$E_{SJ}[n,n_+] = E_J[n,n_+] + \langle \delta v \rangle \int \theta(\vec{r})\,[n(\vec{r}) - n_+(\vec{r})]\, d^3r - \tilde{\epsilon} \int n_+(\vec{r})\, d^3r, \qquad (2)$$

where $\langle \delta v \rangle$ is a constant potential determined for each metal by a bulk stability condition (see below) with the aid of a one-parameter model pseudopotential such as

Ashcroft's empty core, and $\tilde{\epsilon}$ is the jellium self-repulsion per particle. Physically, the last equation means that, starting with jellium, the ions are uniformly localized but that their interaction with the valence electrons is only considered perturbatively and in a spherically averaged way.

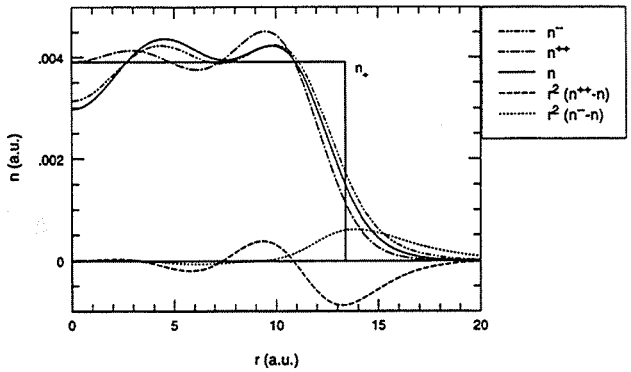

Figure 1: Electronic densities for Na_{40} obtained solving the Kohn-Sham equations in the SJM with fixed background density, within the LDA. Displayed are the densities for the neutral system (n), the double negative system (n^{--}) and the double positive system (n^{++}). Below, we show the radial probability charge density in arbitrary units. The valence-electron density parameter for Na is $r_s^B = 3.93$ bohr.

Stabilized Jellium has similar shell structure to ordinary jellium. However, in contrast with jellium, it yields realistic bulk binding energies and compressibilities as well as realistic surface energies. It may be applied to clusters in two versions: in the first, the jellium background is taken rigid at the same density as the bulk, and, in the second, the jellium background is allowed to relax to its equilibrium position. Defining $E(N, r_s, r_c, z)$ as the total energy of a cluster with N valence electrons, with background density corresponding to the density parameter r_s, pseudopotential core radius r_c and charge z we have in the second version:

$$\frac{\partial}{\partial r_s}\left[\frac{E(N, r_s, r_c, z)}{N}\right]_{r_s=r_s^*} = 0, \tag{3}$$

where the derivative is evaluated at fixed N. In the limit $N \to \infty$ the latter equation is the bulk stability condition which is central to the Stabilized Jellium concept (and which allows to determine r_c and, therefore, $\langle \delta v \rangle$ to be inserted in Eq. (2)). The r_s^* is the valence electron density in the bulk, r_s^B.

The elastic stiffness of the cluster is

$$B^* = B(N, r_s^*, r_c, z) = \frac{1}{12\pi r_s^* N}\frac{\partial^2}{\partial r_s^2}\left[\frac{E(N, r_s, r_c, z)}{N}\right]_{r_s=r_s^*}, \tag{4}$$

which, again in the limit $N \to \infty$, gives the bulk modulus of the solid, B^B.

Let us start with Stabilized Jellium with a fixed positive background. Fig. 1 shows the valence-electron density of neutral Na_{40} compared with the same quantity for Na_{40}^{++}

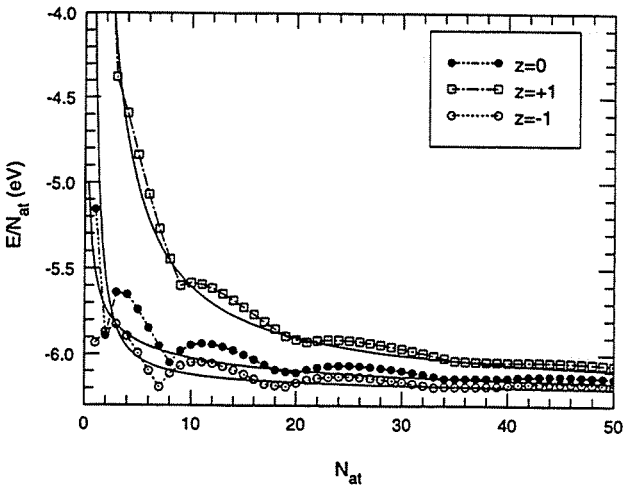

Figure 2: The symbols represent binding energies per atom, as a function of the number of atoms, for neutral sodium clusters ($z = 0$), with a single negative charge ($z = -1$) and a single positive charge ($z = +1$), obtained in the Kohn-Sham - LDA method in the SJM. The continuous curves represent the liquid drop energy. Note that for Na_N^-, with $N < 15$, the Kohn-Sham solutions have a positive upper energy level.

and Na_{40}^{--}. The charge excess lies on the surface, and $r^2(n^{++} - n)$ spreads out over a larger region than $r^2(n^{--} - n)$.

Fig. 2 represents the binding energies per atom for neutral, single positively and negatively charged Na clusters, with the number of atoms $N_{at} = N$ ranging from 2 to 50.

Contrary to some belief, the liquid drop model (LDM) for the electronic fluid, which nicely averages the quantal results, does not have adjustable phenomenological parameters (i.e., all its parameters may be derived from a density functional such as (1) or (2)). It may be written [5] as

$$E_{LDM}(N,z) = a_v N + a_s N^{\frac{2}{3}} + a_c N^{\frac{1}{3}} + z\,W + \frac{z}{r_s}\left(c + \frac{z}{2}\right) N^{-1/3} + O(N^{-2/3}), \tag{5}$$

where a_v is the binding energy per particle in the bulk, a_s is the surface energy coefficient, a_c is the curvature energy coefficient [6], W is the work function, c describes a quantal size effect to the work function (this is $c \simeq -0.08$ for all metals [7] and not $c = -1/8$, as an early erroneous theoretical prediction and some fits to experimental data might have suggested). N refers here to the number of valence electrons in the neutral cluster and not the number of valence electrons in the charged custer (e.g., in Na_{40}^{++}, we have $N = 40$ and $z = 2$, while, in Al_{18}^{--}, we have $N = 3 \times 18 = 54$ and $z = -2$). Note that in the literature z refers to the number of excess electrons, i.e., the symmetric of the charge, and not to the charge as here.

The ionization energy, which is easily obtained in the Kohn-Sham scheme subtract-

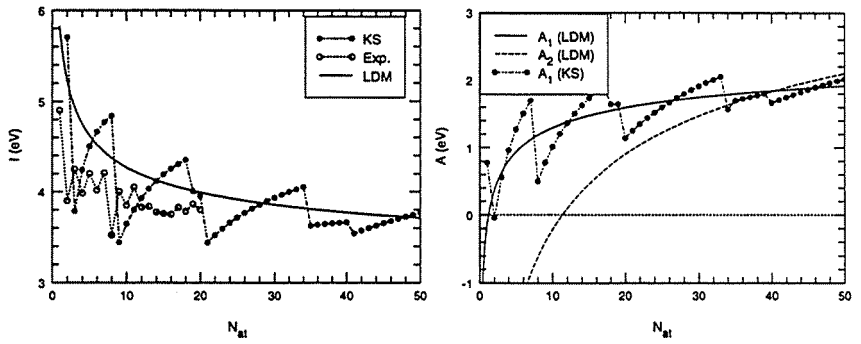

Figure 3: First ionization energy (left) and first electronic affinity (right) for sodium clusters as a function of the number of atoms, in the framework of the SJM, solving the Kohn-Sham equations in the LDA and using the LDM. The work function in the SJM is 2.92 eV (the experimental value is 2.75 eV). The experimental results (Exp.) for the ionization energy are taken from Ref. 8. On the right the second affinity in the LDM is also shown.

ing the total energy of the charged system by that of the neutral system, is compared with experimental data in Fig. 3. The electronic shell structure shows up in "jumps" at shell closures (which give the magic numbers...). The same effect is seen for the electronic affinity. The spherical shape (in stabilized jellium as in jellium) shows a much too pronounced shell structure, but it is well known that allowance for deformation reduces the fluctuations. The liquid drop ionization energy and affinity are easily derived from Eq. (5) giving

$$I(N) = E(N,-1) - E(N,0) = -W - (c - \frac{1}{2})\frac{1}{R+d_s} \quad (6)$$

$$A(N) = E(N,0) - E(N,1) = -W - (c + \frac{1}{2})\frac{1}{R+d_s}, \quad (7)$$

where, for convenience in describing the smallest clusters, we have added a d_s term to the radius ("spill out" effect of the charge with respect to the jellium edge). The LDM is unable to reproduce the shell structure since it represents a semiclassical approximation. The liquid drop values lie above the ionization data for small clusters and approach asymptotically the SJM work function, which is only slightly higher than the experimental one.

All the results shown up to now refer to a non-self compressed jellium background. Self-compression reduces the cluster radius and allows for the evaluation of the elastic stiffness (this may be larger than in the bulk). They hardly change anything in the shell structure. Figs. 4 and 5 represent self-compression effects for neutral and double positively charged Na and Al clusters.

Neutral metal clusters suffer self-compression, $r_s^*/r_s^B < 1$, an effect which is easily understood in terms of surface tension [9]. This compression is bigger for smaller clusters than for larger ones (for any chemical species), and more pronounced for aluminum (higher density) than for sodium (lower density) clusters. Shell effects are visible in

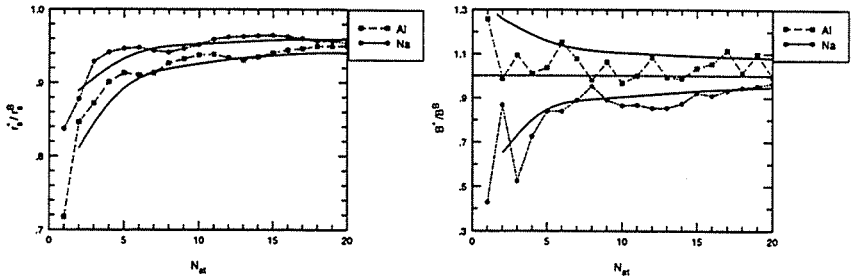

Figure 4: On the left, ratio between the ionic density parameter and its bulk value, r_s^*/r_s^B, in the framework of the Kohn-Sham - LDA approach to the Stabilized Jellium Model, for neutral aluminum ($r_s^B = 2.07$ bohr, valence 3) and sodium clusters ($r_s^B = 3.93$ bohr, valence 1) with N_{at} atoms. The full curves refer to the LDM results. On the right, ratio between the elastic stiffness of the cluster and the bulk modulus of the solid.

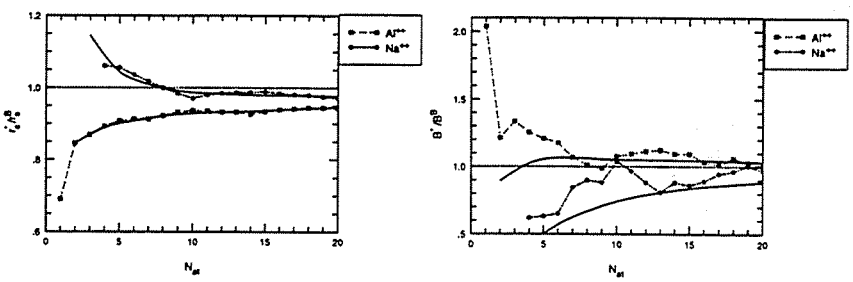

Figure 5: Same as Fig. 4 for double positively charged aluminum and sodium clusters.

local minima for r_s^* and local maxima for B^*. Again, the LDM gives a good average behavior and allows us to see the asymptotic behavior. For example, for big clusters, r_s^* approaches r_s^B in the following way:

$$r_s^* = r_s^B(1 - \beta N^{-1/3}), \tag{8}$$

with β a coefficient depending on the metal. The elastic stiffness of Na approaches the bulk limit from below while the Al one approaches that limit from above (this fact may be interesting for the production of hard, nanostructured materials).

Uncompensated charge reduces the self-compression effect and may even originate self-expansion, when the charge is big enough to overcome surface tension [10]. Small Na_N^{++} clusters show self-expansion up to the size N=8, and a small self-compression for bigger sizes. On the contrary, Al_N^{++} clusters are always self-compressed. Na_N^{++} clusters are softer while Al_N^{++} are harder than the solid. In general, the role of charge consists in softening the clusters.

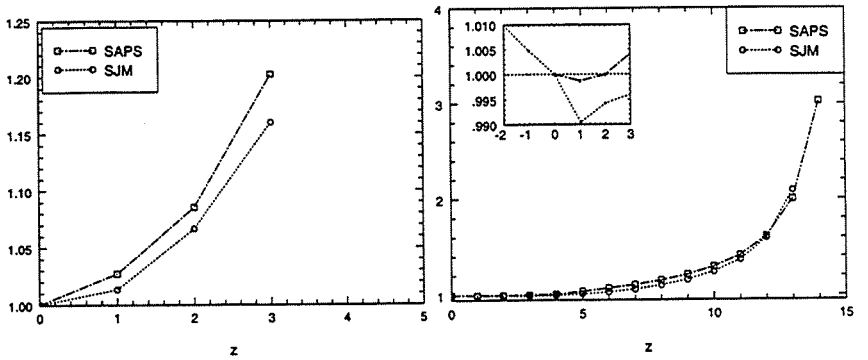

Figure 6: Ionic density parameter r_s^* for Na_8^{z+} (left) and Al_8^{z+} (right), normalized to that of the neutral cluster, in the SJM, as a function of charge z. Also represented is the radius of the outer ionic shell of the same clusters normalized to that of the neutral system in the SAPS. The inset shows a small but somewhat strange phenomenon: the aluminum cluster size decreases in both models (the lower curve refers to the SJM) when a single charge is added.

3. ATOMISTIC MODELS: SAPS AND *AB INITIO* PSEUDOPOTENTIAL DENSITY FUNCTIONALS

The density functional of the SAPS [11], a model which has been developped and applied mostly by the Valladolid school, may be written as

$$E_{SAPS}([n],\vec{R}_i) = T_s[n] + E_{xc}[n] + 4\pi \int dr\, r^2 v_{ext}(r)\, n(r) + \tfrac{1}{2}\int d^3r \int d^3r' \frac{n(\vec{r})n(\vec{r'})}{|\vec{r}-\vec{r'}|} + \tfrac{1}{2}\sum_{i\neq j}^{N} \frac{z_i z_j}{|\vec{R}_i - \vec{R}_j|}, \quad (9)$$

where z_i is the charge of ion i. Now $v_{ext}(\vec{r}) = \left\langle \sum_i w(\vec{r}-\vec{R}_i) \right\rangle$, with w the pseudopotential, is a potential average around the cluster center. For the pseudopotential we have used the recently proposed evanescent core pseudopotential [12], which gives very good bulk properties. The repulsion between the ionic cores has been approximated by an interaction between point charges (last term of Eq. (9)). In this model the ions are allowed to go to their equilibrium positions (considering forces given by the Feynman-Hellman theorem) but the spherical average, which is very useful to decrease the computational burden of the calculation, gives rise to unrealistic ionic spherical shells.

Notwithstanding the complexity increase, the SAPS gives some results close to those of the Stabilized Jellium Model with self-compression [13]. Fig. 6 illustrates a striking similarity of SAPS with Stabilized Jellium: the systems "explode" in the same way when the charge is increased.

However, for other properties, the SAPS and the SJM differ. A problem of SAPS is that the spherical approximation seems to be too restrictive to correctly describe the electronic binding energies: these turn out to be too high and, therefore, the cohesive energies turn out to be too low in comparison with experiment [13]. Due to a

cancellation of errors the simpler SJM gives better cohesive energies.

Finally, the density functional for the "Ab Initio" Pseudopotential Model, using a local pseudopotential w (appropriate for Na), may be written as

$$E_{AIPM}([n],\vec{R}_i) = T_s[n] + E_{xc}[n] + \int d^3r n(\vec{r}) \sum_i w(\vec{r}-\vec{R}_i) \\ +\tfrac{1}{2}\int d^3r \int d^3r' \tfrac{n(\vec{r})n(\vec{r'})}{|\vec{r}-\vec{r'}|} + \tfrac{1}{2}\sum_{i\neq j}^{N} \tfrac{z_i z_j}{|\vec{R}_i-\vec{R}_j|} \,. \qquad (10)$$

A more complicated third term arises when non-local pseudopotentials are used.

To solve the corresponding Kohn-Sham equations it is convenient in solid-state calculations to choose a momentum-space representation [14]. In this case a plane-wave expansion of the orbitals is employed. If we use this method to perform cluster calculations, translation invariance has to be artificially introduced. This is done enclosing the cluster in a large cell (supercell) and duplicating it in a periodic lattice. Care must be taken in order that the supercell is large enough to minimize the interactions between the periodic images of the cluster. The method is, arguably, the best method available for "ab-initio" calculations on not very small clusters (for the smaller ones, an expansion in a Gaussian basis may be the method of choice). The equilibrium ionic positions ($\vec{R}_i$) may be obtained with standard molecular dynamics techniques.

However, a problem arises when one wants to simulate charged clusters: a huge supercell is required by the long-range Coulomb interaction between the *charged* images. To circumvent this difficulty one can shield each cluster with a spherical shell charge distribution with total charge chosen to make the supercell neutral. If this charge is suitably placed in order to lead to a null total electric dipole, one is left only with quadrupolar interactions between the periodic images of the system composed of the shell charge and the charged cluster. To obtain correct results it suffices then to subtract, after each self-consistency cycle, the spurious interactions of the cluster with the shell charge distribution (if the shell is thin and its radius is large enough, this amounts to a constant).

The output for the cohesive energy of neutral clusters obtained with the plane-wave method improves on SAPS results of Ref. 13, in comparison with experiment (see Table 1). The SJM results are very good. We have also confirmed the reduction of bond lengths predicted by the SJM with self-compression and also shown by experiment (this was also done in Ref. 15 but using a Linear Combination of Atomic Orbitals method). The ionization energies in the AIPM are better than the SJM values.

Bond lengths for charged clusters are shown in Table 2. Note their increase with respect to the values in Table 1. Further results on charged clusters are reported in Ref. 18.

4. CONCLUSIONS

We have examined charged clusters taking different approximations for the ions. Although the properties of simple metals are mostly due to the valence electrons and simple approximations hold reasonably well, the treatment of the ions in models of increasing complexity improves, in general, the agreement with the data, exhibiting in a more precise way the role of the ions. However, this is not always the case: for

Bond lengths					Cohesive energies				Ionization energies			
Cluster	PW	G	SJM	Exp	PW	G	SJM	Exp	PW	G	SJM	Exp
Na_2	5.5	5.5	6.21	5.83	0.67	0.45	0.73	0.31	5.50	5.1	5.70	4.9
Na_3	6.1	6.2	6.60	–	0.60	0.43	0.49	0.45	3.88	4.0	3.78	3.9
Na_6	6.3	6.0	6.75	–	0.83	0.73	0.69	0.63	4.57	4.4	4.66	4.2

Table 1: Equilibrium atomic distances (left), cohesive energies (center) and ionization energies (right) for dimers, equilateral trimers and regular octahedral hexamers of Na. Atomic distances are given in bohr and energies in eV. Shown are results from pseudopotential plane-wave calculations (PW), pseudopotential Gaussian-basis calculations (G, Ref. 16), SJM (with self-compression, except for the ionization energies) and experiment (Refs. 8, 19, 20 for bond lenghts, cohesive and ionization energies, respectively). The non-local pseudopotential employed was the Bachelet, Hamann and Schlüter form of Ref. 17. The Gaussian-basis atomic distances for the trimer and hexamer are average values since the calculated minimum energy geometries of Ref. 16 are not regular structures.

Bond lengths			
Cluster	PW	G	SJM
Na_2^+	6.8	6.4	7.04
Na_3^+	6.2	6.0	6.59
Na_6^+	6.5	-	6.87

Table 2: Equilibrium atomic distances, in bohr, for dimers, equilateral trimers and regular octahedral hexamers of Na^+. PW and G as in Table 1. Again, average bond length values are shown for G.

instance, the lack of improvement of the SAPS with respect to SJM cohesive energies speaks for the necessity of allowing for realistic ionic geometries.

Further work remains to be done for charged clusters, in particular with "ab initio" techniques. Problems like, e. g., systematics of physical properties for clusters with increasing size, structures and isomerism, limits of stability, further applications of the liquid drop formula, and effects of non-locality in exchange and correlation present challenges which should be tackled both with atomistic methods and continuous models for the ionic structure: if the first give more accuracy, the second are more convenient for computational purposes and physical understanding.

ACKNOWLEDGEMENTS

We are very grateful to J. L. Martins (INESC, Lisbon, Portugal), V. Torres (University of Aveiro, Portugal), L. C. Balbás and B. Torres (University of Valladolid, Spain), and J. P. Perdew and M. Seidl (Tulane University, New Orleans, USA) for their collaboration in parts of the work reported here. This work has been partially supported by the Portuguese PRAXIS XXI program (Project 2/2.1/FIS/26/94) and by the

Junta Nacional de Investigação Científica e Tecnológica (Project PBIC/C/FIS/2216/95).

REFERENCES

[1] R. M. Dreizler and E. K. U. Gross, *Density Functional Theory* (Springer, Berlin, 1990).

[2] J. P. Perdew, in these Proceedings.

[3] M. Brack, *Rev. Mod. Phys.* **65** (1993) 677.

[4] J. P. Perdew, H. Q. Tran, and E. D. Smith, *Phys. Rev. B* **42** (1990) 11627; M. Brajczewska, C. Fiolhais, and J. P. Perdew, *Int. J. Quantum Chem.* **S27** (1993) 249; A. Vieira, PhD. Thesis, Coimbra, 1997.

[5] M. Seidl and M. Brack, *Annals of Physics (N.Y.)* **245** (1996) 275; M. Seidl and J. P. Perdew, *Phys. Rev. B* **50** (1994) 5744.

[6] C. Fiolhais and J. P. Perdew, *Phys. Rev. B* **45** (1992) 6207.

[7] M. Seidl, J. P. Perdew, M. Brajczewska, and C. Fiolhais, *Phys. Rev. B* **55** (1997) 13288; M. Seidl, J. P. Perdew, M. Brajczewska, and C. Fiolhais, submitted.

[8] M. M. Kappes, M. S. Schär, U. Röthlisberger, Ch. Yeretzian, and E. S. Chumacher, *Chem. Phys. Lett.* **143** (1988) 251.

[9] J. P. Perdew, M. Brajczewska, and C. Fiolhais, *Solid State Commun.* **88** (1993) 795.

[10] A. Vieira, M. Brajczewska, C. Fiolhais, and J. P. Perdew, *Int. J. Quantum Chem.* **60** (1996) 1537; M. Brajczewska, A. Vieira, C. Fiolhais, and J. P. Perdew, *Prog. Surf. Science* **53** (1996) 315.

[11] M. P. Iñiguez, M. J. López, J. A. Alonso, and J. M. Soler, *Z. Phys. D* **13** (1989) 171.

[12] C. Fiolhais, J. P. Perdew, S. Q. Armster, J. MacLaren, and M. Brajczewska, *Phys. Rev. B* **51** (1995) 14001; erratum *ibid.* **53** (1996) 13193.

[13] A. Vieira, B. Torres, C. Fiolhais, and L. C. Balbás, *J. Phys. B* **30** (1997) 3583.

[14] J. Ihm, A. Zunger, and M. L. Cohen, *J. Phys. C: Solid State Phys.* **12** (1979) 4409.

[15] F. Nogueira, C. Fiolhais, J. He, J. P. Perdew, and A. Rubio, *J. Phys.: Condens. Matter* **8** (1996) 287.

[16] J. L. Martins, J. Buttet, and R. Car, *Phys. Rev. B* **31** (1985) 1804.

[17] G. S. Bachelet, D. R. Hamann, and M. Schluter, *Phy. Rev. B* **26** (1982) 4199.

[18] F. Nogueira, J. L. Martins, J. M. Pacheco, and C. Fiolhais, to be published.

[19] C. Fiolhais, F. Nogueira, and C. Henriques, *Prog. Surf. Science* **53** (1996) 315.

[20] C. Bréchignac, Ph. Cahuzac, J. Leygnier, and J. Weiner *J. Chem. Phys.* **90** (1989) 1492.